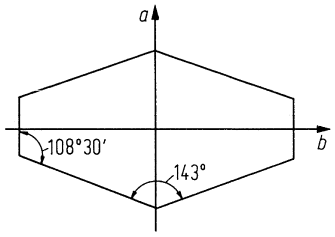

Fig. 31A-4-001. $RbH_3(SeO_3)_2$. Crystal form [69Shu].

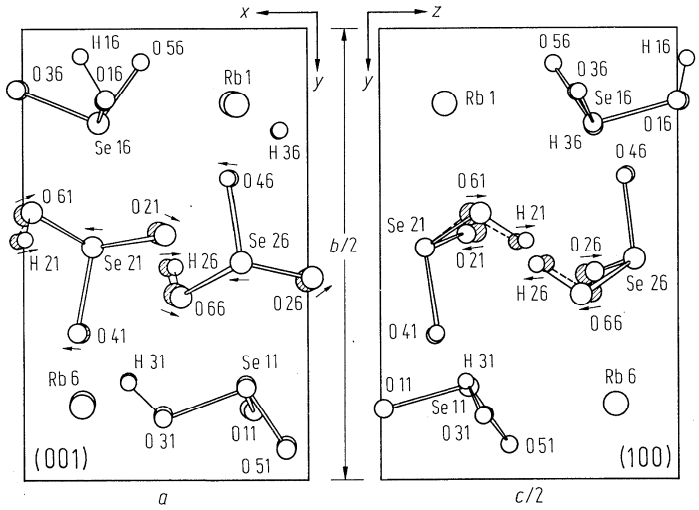

Fig. 31A-4-002. $RbH_3(SeO_3)_2$. Crystal structure of phase II [78Gri1]. Projections on (001) and (100). Shaded atoms represent the even structure which is obtained by an assumption that the super lattice reflections are not observed. The arrows show the major displacements due to the phase transition.

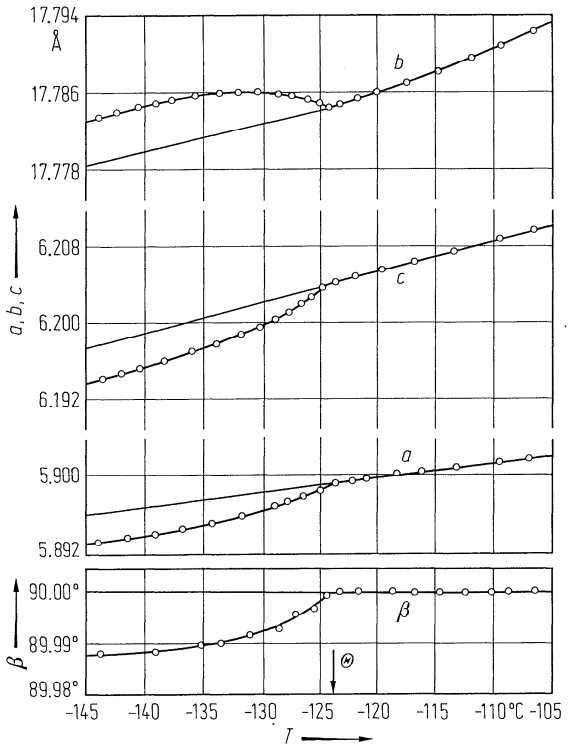

Fig. 31A-4-003. $RbH_3(SeO_3)_2$. a, b, c, β vs. T [78Kob].

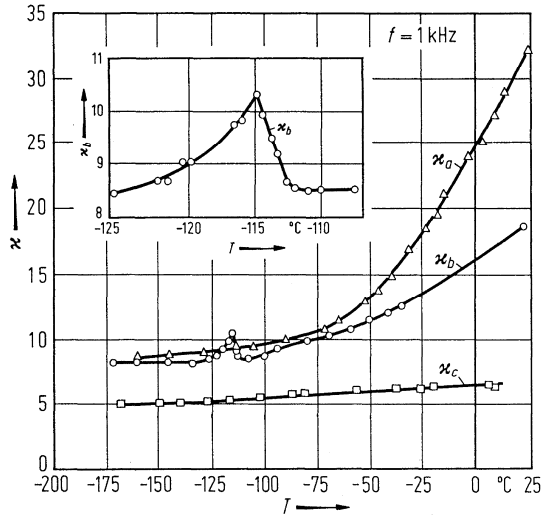

Fig. 31A-4-004. $RbH_3(SeO_3)_2$. κ_a, κ_b, κ_c vs. T [69Shu].

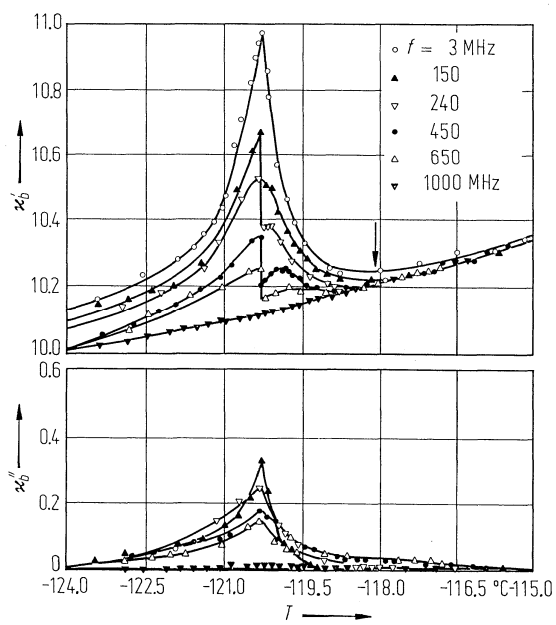

Fig. 31A-4-005. $RbH_3(SeO_3)_2$. κ_b', κ_b'' vs. T [80Tsu]. Parameter: f. Arrow indicates the I′–I phase transition temperature.

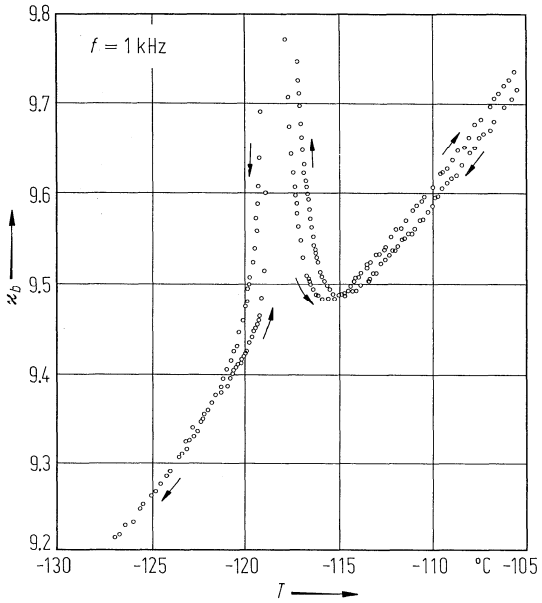

Fig. 31A-4-006. $RbH_3(SeO_3)_2$. κ_b vs. T for a homogeneous crystal [80Got2].

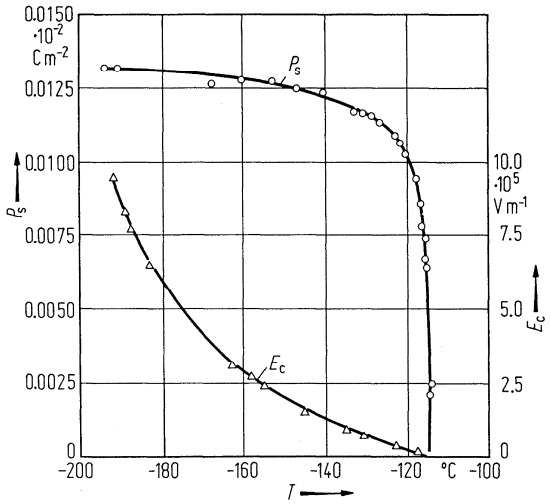

Fig. 31A-4-007. $RbH_3(SeO_3)_2$. P_s, E_c vs. T [69Shu].

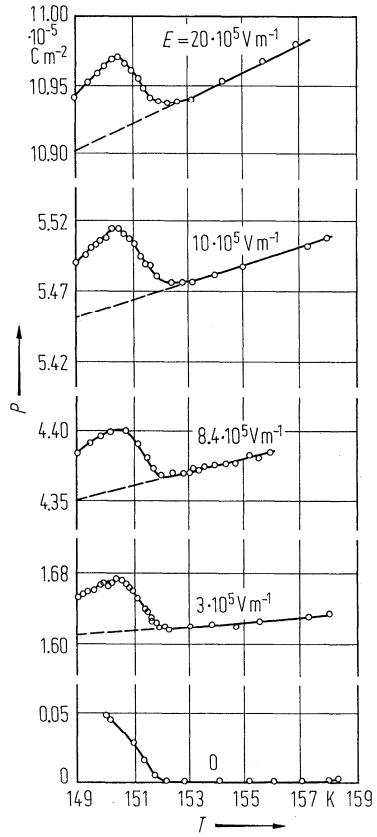

Fig. 31A-4-008. $RbD_3(SeO_3)_2$. P vs. T [76Gla1]. Parameter: E.

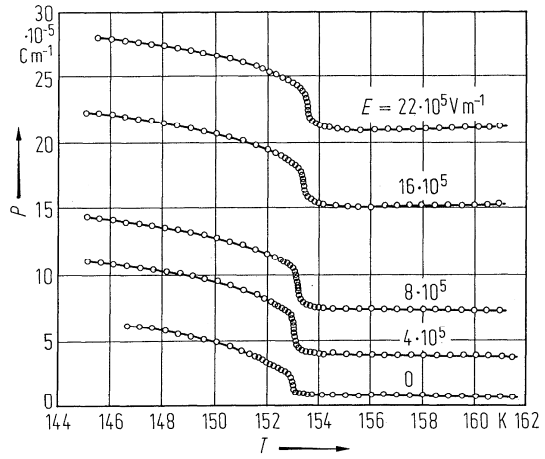

Fig. 31A-4-009. $RbH_3(SeO_3)_2$. P vs. T [76Gla2]. Parameter: E.

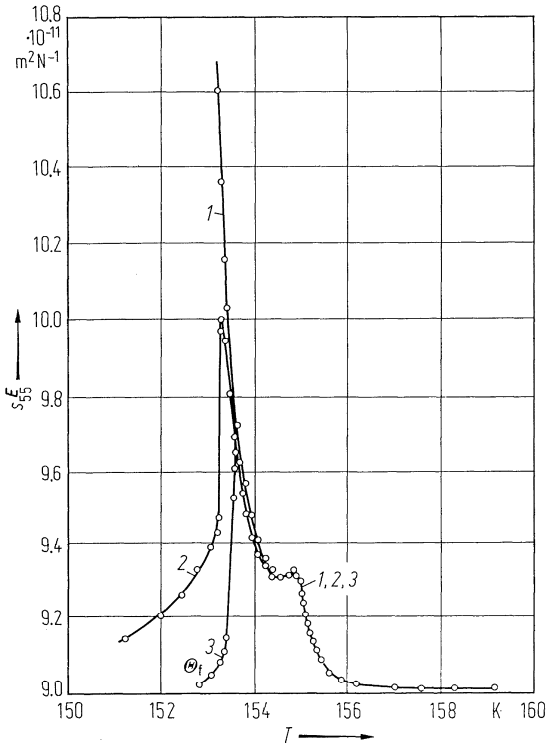

Fig. 31A-4-010. $RbH_3(SeO_3)_2$. s_{55}^{E} vs. T [77Gla]. Parameter: E_{bias}. Curve *1*: E_{bias} = 0; *2*: $1 \cdot 10^3$ kV m^{-1}; *3*: $2.2 \cdot 10^3$ kV m^{-1}.

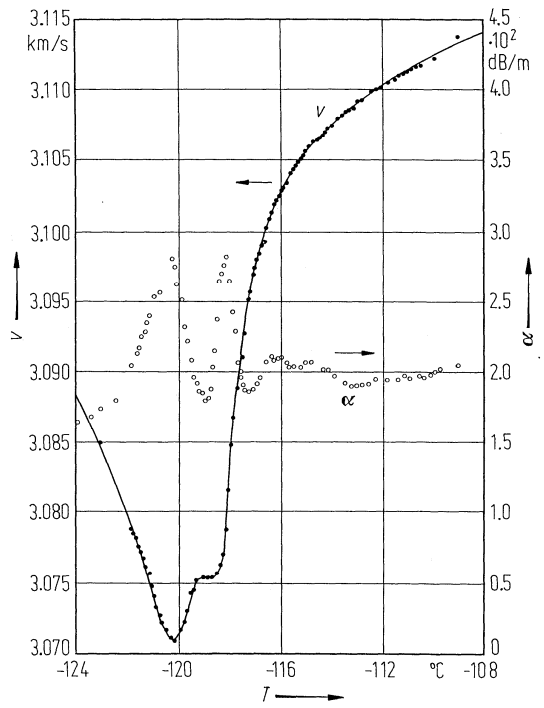

Fig. 31A-4-011. $RbH_3(SeO_3)_2$. v, α vs. T [80Tak]. v: velocity of the longitudinal sound propagated along the c axis. α: attenuation coefficient. f = 10 MHz.

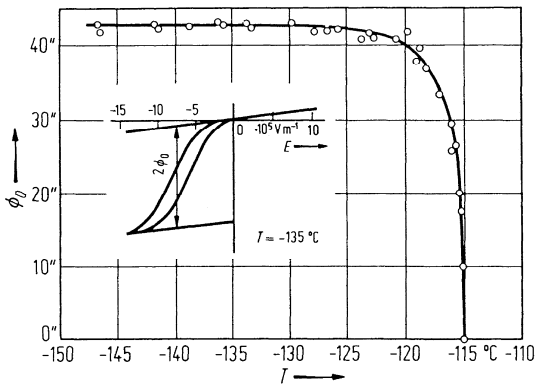

Fig. 31A-4-012. $RbH_3(SeO_3)_2$. ϕ_0 vs. T, and electrooptical hysteresis loop [70Iva]. ϕ_0: angle of rotation of the optical indicatrix around the b axis.

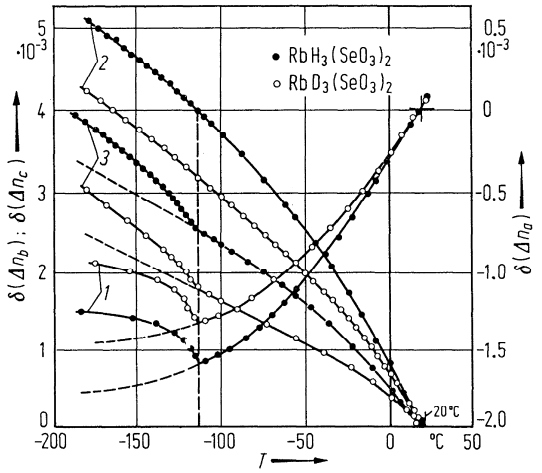

Fig. 31A-4-013. $RbH_3(SeO_3)_2$, $RbD_3(SeO_3)_2$. $\delta(\Delta n)$ vs. T [70Iva]. $\delta(\Delta n) = [\Delta n]_T - [\Delta n]_{20\ °C}$. Curves *1*: Δn_a, birefringence observed along the *a* axis; *2*: Δn_b, along the *b* axis; *3*: Δn_c, along the *c* axis. At $\lambda = 632.8$ nm.

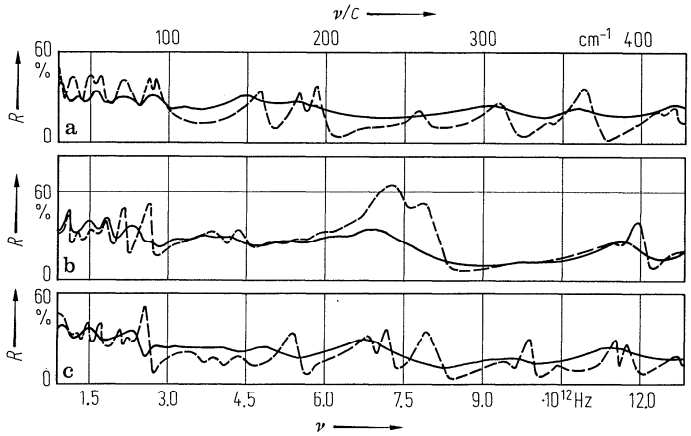

Fig. 31A-4-014. $RbH_3(SeO_3)_2$. R vs. ν [73Pet]. R: reflectivity for the far infrared radiation polarized along (**a**) X axis, (**b**) Y axis, and (**c**) Z axis. The solid curves are at 25 °C and the dashed curves are at –170 °C.

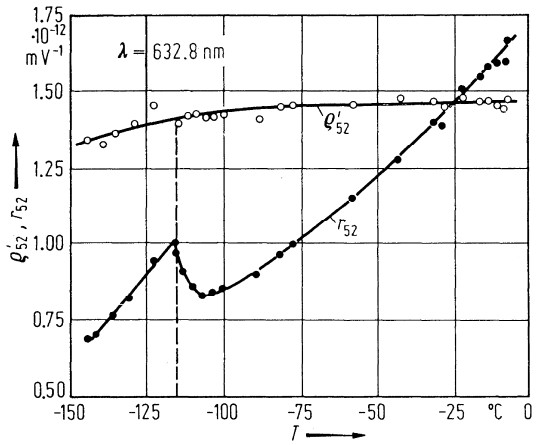

Fig. 31A-4-015. $RbH_3(SeO_3)_2$. r_{52}, ρ'_{52} vs. T [70Iva]. r_{52}: electrooptic constant for E, $\rho'_{52} = r_{52} \cdot 4\pi\,(\kappa_2 - 1)^{-1}$.

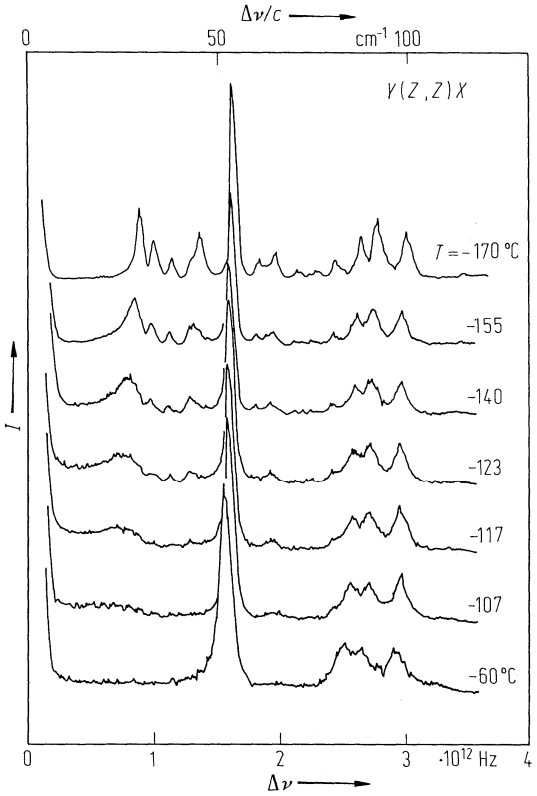

Fig. 31A-4-016. $RbH_3(SeO_3)_2$. I vs. $\Delta\nu$ [80Sak]. $\Delta\nu$: Raman shift. Parameter: T.

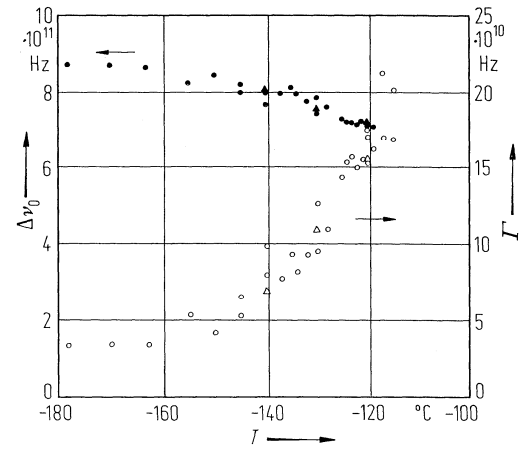

Fig. 31A-4-017. $RbH_3(SeO_3)_2$. $\Delta\nu_0$ and Γ vs. T [80Sak]. $\Delta\nu_0$: Raman peak frequency of the lowest A_1-mode. Γ: line width of the mode defined as halfwidth on the high frequency side at half-maximum. Circles and triangles are data measured in geometries of $Y(ZZ)X$ and $XY(ZZ)XY$, respectively.

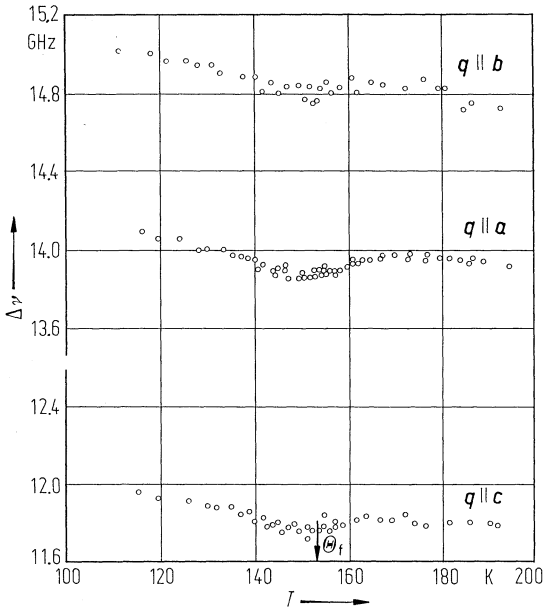

Fig. 31A-4-018. $RbH_3(SeO_3)_2$. $\Delta\nu$ vs. T [83Sak]. $\Delta\nu$: Brillouin frequency shift. Parameter: direction of the wave vector $\boldsymbol{q}$ of an acoustic phonon. $\lambda = 514.5$ nm.

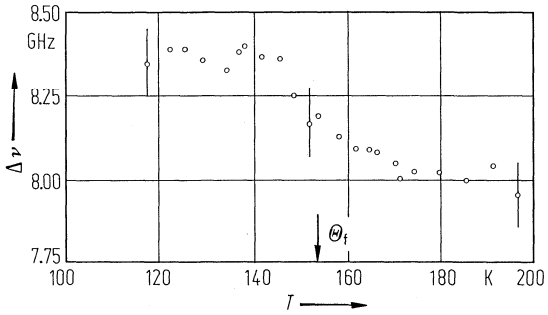

Fig. 31A-4-019. $RbH_3(SeO_3)_2$. $\Delta\nu$ vs. T [83Sak]. $\Delta\nu$: Brillouin frequency shift for the c_{55} mode. $\lambda = 514.5$ nm.

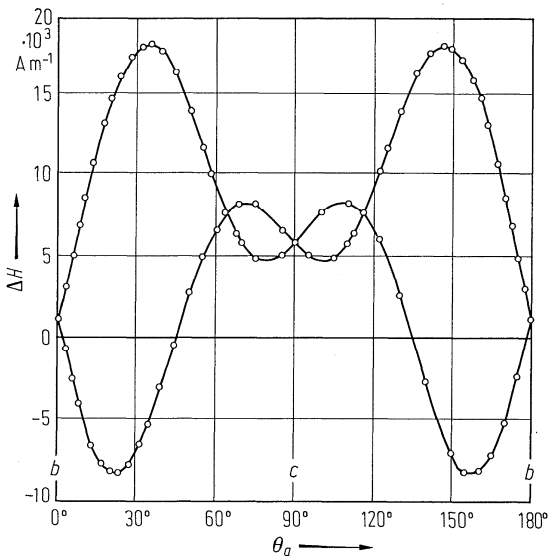

Fig. 31A-4-020. $RbH_3(SeO_3)_2$. ΔH vs. θ_a [79Tak]. $\Delta H = H_R - H_L$, where H_R and H_L are the resonance field of ^{87}Rb with and without quadrupole interaction, respectively. $f = 8$ MHz, $T = 13$ °C. θ_a: angle of rotation around the *a* axis.

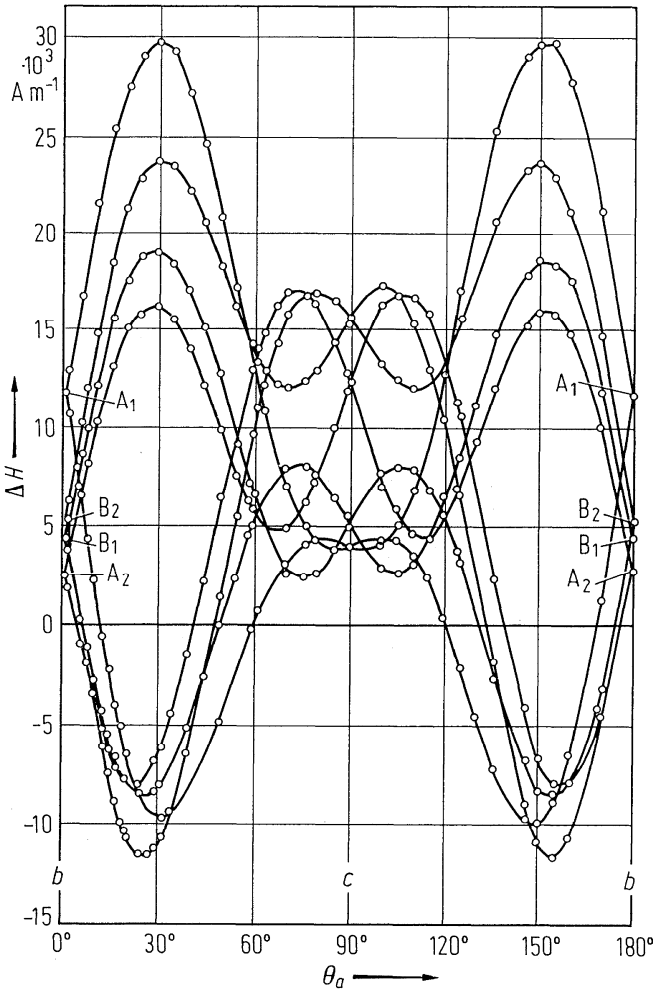

Fig. 31A-4-021. $RbH_3(SeO_3)_2$. ΔH vs. θ_a [79Tak]. $\Delta H = H_R - H_L$, where H_R and H_L are the resonance field of ^{87}Rb with and without quadrupole interaction, respectively. f = 8 MHz, T = –155.5 °C. θ_a: angle of rotation around the a axis.

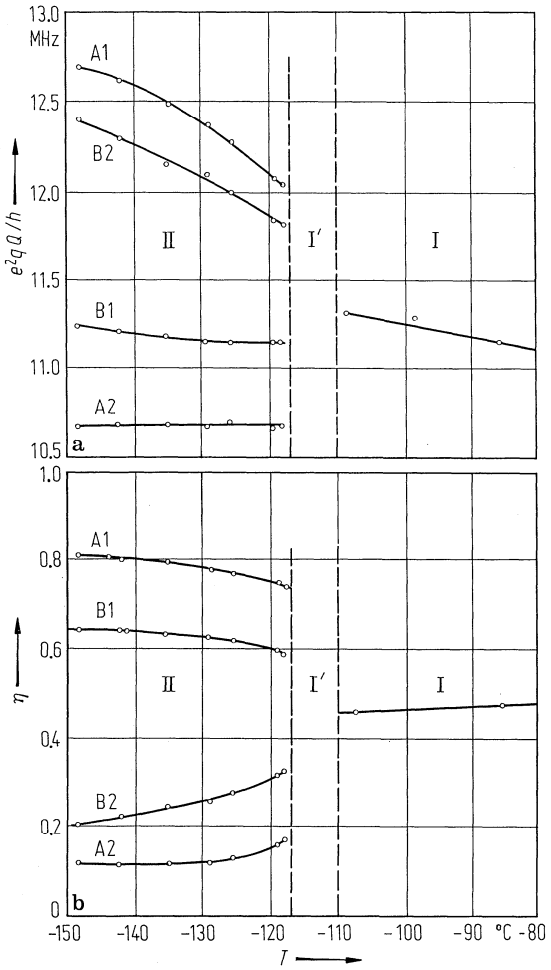

Fig. 31A-4-022. $RbH_3(SeO_3)_2$. (**a**) e^2qQ/h vs. T, (**b**) η vs. T. ^{85}Rb NMR [83Sel].

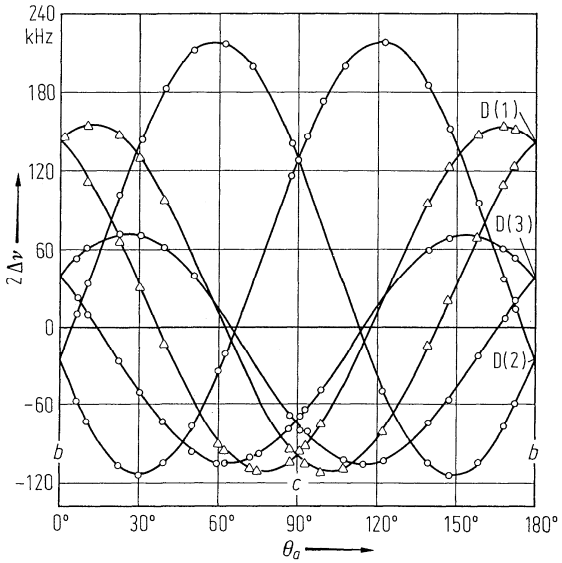

Fig. 31A-4-023. $RbD_3(SeO_3)_2$. $2\Delta\nu$ vs. θ_a [79Shi]. $2\Delta\nu = \nu(m = 1 \leftrightarrow 0) - \nu(m = 0 \leftrightarrow -1)$: frequency difference between the quadrupole-split pair lines of deuterons for the *a* axis rotation. $T = 14$ °C. See also Fig. 31A-4-024; Table 31A-4-005. θ_a: angle of rotation around the *a* axis.

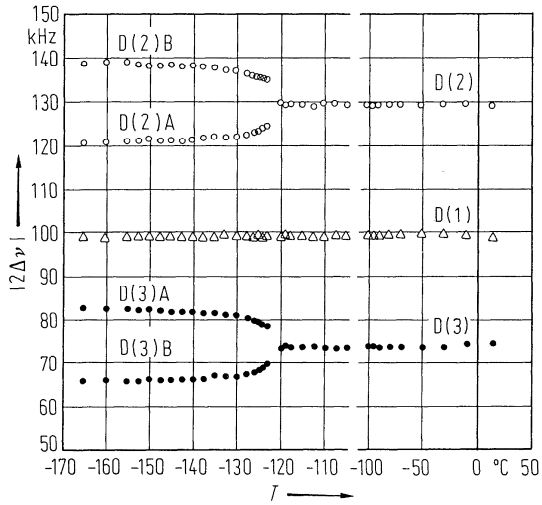

Fig. 31A-4-024. $RbD_3(SeO_3)$. $|2\Delta\nu|$ vs. T [79Shi]. $2\Delta\nu = \nu(m = 1 \leftrightarrow 0) - \nu(m = 0 \leftrightarrow -1)$: frequency difference between the quadrupole-split pair lines for the *a* axis rotation. $\boldsymbol{H} \parallel \boldsymbol{c}$. See also Fig. 31A-4-023; Table 31A-4-005.

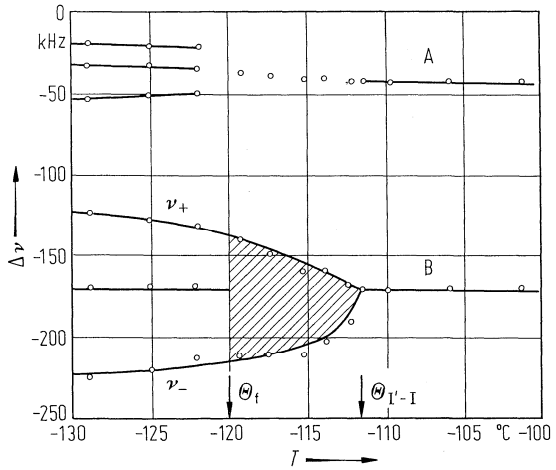

Fig. 31A-4-025. $RbD_3(SeO_3)_2$. $\Delta\nu$ vs. T [82Bli]. $\Delta\nu$: second-order quadrupole shifts of the central 1/2 ↔ – 1/2 ^{87}Rb NMR transition. $\boldsymbol{H} \perp \boldsymbol{b}$. $\angle$ ($\boldsymbol{H}$, $\boldsymbol{c}$) = 40°. ν_L = 29.5 MHz. Hatched region indicates a broad continuous spectrum.

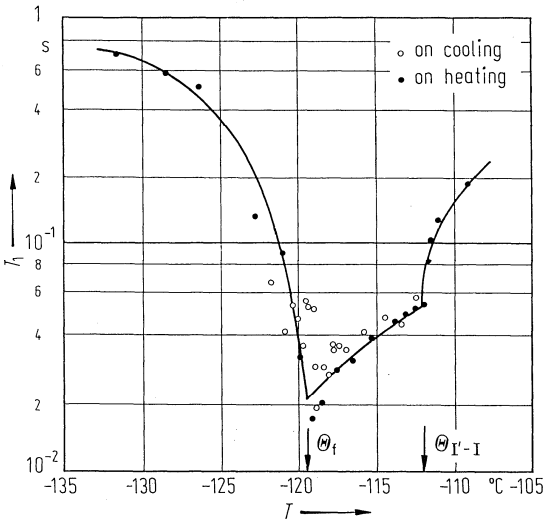

Fig. 31A-4-026. $RbD_3(SeO_3)_2$. T_1 vs. T [82Bli]. T_1: ^{87}Rb spin-lattice relaxation time. $\boldsymbol{H} \perp \boldsymbol{a}$. $\angle$ ($\boldsymbol{H}$, $\boldsymbol{b}$) = 30°. f = 88.5 MHz.

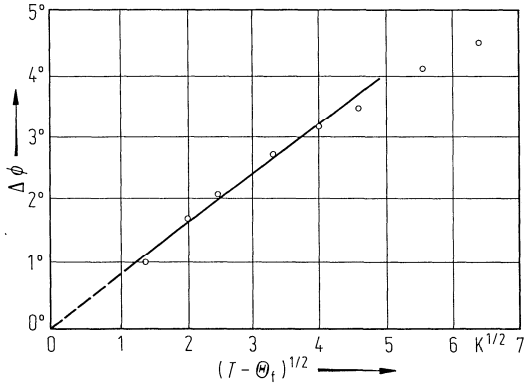

Fig. 31A-4-027. $RbH_3(SeO_3)_2$. $\Delta\phi$ vs. $(T - \Theta_f)^{1/2}$ [80Jer]. $\Delta\phi$: rotation angle of the $(SeO_3)_{II}$ groups.

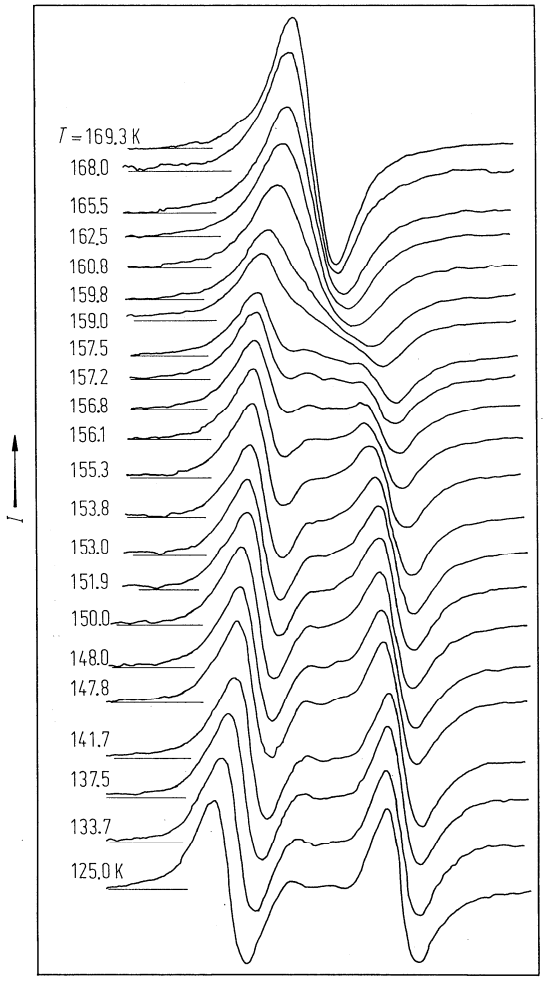

Fig. 31A-4-028. $RbH_3(SeO_3)_2$. ESR line shapes for Cr^{3+} [82Tak]. Parameter: T. $\boldsymbol{H} \perp \boldsymbol{a}$. $\angle(\boldsymbol{H}, \boldsymbol{b}) = 75°$. $f = 9$ GHz.

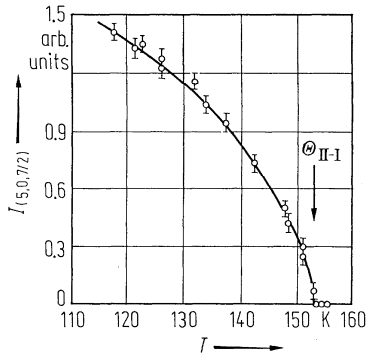

Fig. 31A-4-029. $RbH_3(SeO_3)_2$. $I_{(5,\,0,\,7/2)}$ vs. T [74Mak]. I: integrated intensity of X-ray diffraction.

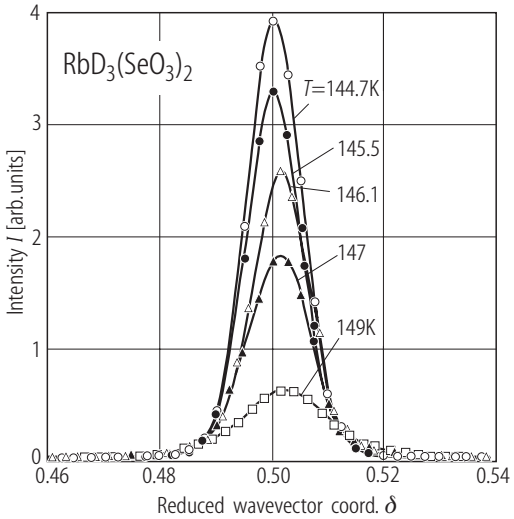

Fig. 31A-4-030. $RbD_3(SeO_3)_2$. I vs. δ at various temperatures [80Ges]. I: intensity of satellite reflection around (2, 0, 0.5) in the (2, 0, δ)-scan.

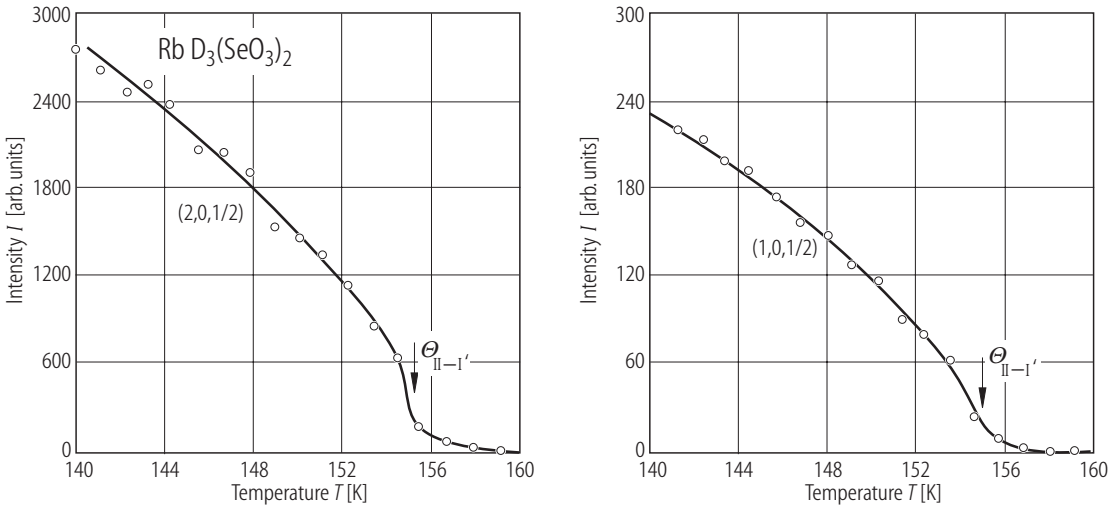

Fig. 31A-4-031. $RbD_3(SeO_3)_2$. *I* vs. *T* [87Mar]. *I*: peak intensity of two incommensurate reflections (2, 0, 0.5) and (1, 0, 0.5).

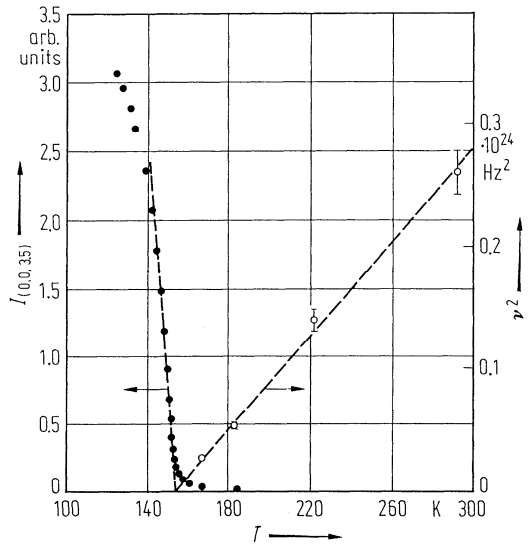

Fig. 31A-4-032. $RbD_3(SeO_3)_2$. $I_{(0,\,0,\,3.5)}$, ν^2 vs. *T* [78Gri2]. $I_{(0,\,0,\,3.5)}$: intensity of superlattice neutron diffraction peak at (0, 0, 3.5). ν: soft mode frequency at the Z-point.

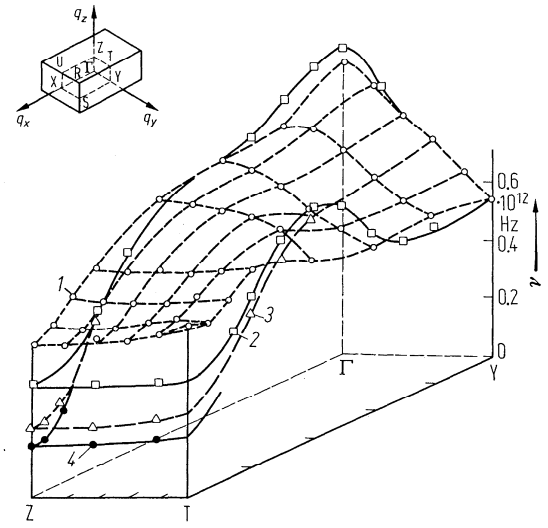

Fig. 31A-4-033. $RbD_3(SeO_3)_2$. Dispersion surface in the q_y–q_z plane at various temperatures [78Gri2]. Insert shows the Brillouin zone. Curve *1*: T = 293 K; *2*: 222 K; *3*: 182 K; *4*: 166 K.